TISSUE ENGINEERING: Part A
Volume 16, Number 12, 2010

DOI: 10.1089/ten.tea.2010.0103

Mechanical and Biochemical Assessments of Three-Dimensional Poly(1,8-Octanediol-*co*-Citrate) Scaffold Pore Shape and Permeability Effects on *In Vitro* Chondrogenesis Using Primary Chondrocytes

Claire G. Jeong, Ph.D.,[1] and Scott J. Hollister, Ph.D.[1–3]

Poly(1,8-octanediol-*co*-citrate) (POC) is a biocompatible, biodegradable elastomer with potential application for soft tissue applications such as cartilage. For chondrogenesis, permeability is a scaffold design target that may influence cartilage regeneration. Scaffold permeability is determined by many factors such as pore shape, pore size, pore interconnectivity, porosity, and so on. Our focus in this study was to examine the effects of pore shape and permeability of two different POC scaffold designs on matrix production, mRNA gene expression, and differentiation of chondrocytes *in vitro* and the consequent mechanical property changes of the scaffold/tissue constructs. Since type I collagen gel was used as a cell carrier in the POC scaffolds, we also examined the effects of collagen gel concentration on chondrogenesis. We found that lower collagen I gel concentration provides a favorable microenvironment for chondrocytes promoting better chondrogenic performance of chondrocytes. With regard to scaffold design, low permeability with a spherical pore shape better enhanced the chondrogenic performance of chondrocytes in terms of matrix production, and mRNA gene expressions *in vitro* compared to the highly permeable scaffold with a cubical pore shape.

Introduction

The field of tissue engineering continues to advance with the discovery of new biomaterials, growth factors, and scaffold fabrication techniques. The use of biodegradable scaffolds as a template on which cells differentiate, proliferate, and grow new tissues has been crucial in the recent advances of cartilage tissue engineering. However, there is still no definitive conclusion as to how scaffold design factors affect chondrogenesis. The choice of scaffold material and geometry will determine the effective scaffold structural and mass transport properties that can significantly influence cartilaginous tissue regeneration. The structural, mechanical, and mass transport properties of scaffolds are determined by combination of many factors such as pore size, pore shape, porosity, pore interconnectivity, permeability, scaffold surface area, scaffold effective stiffness, and scaffold material. These factors cannot be rigorously controlled unless scaffolds are designed with specific architecture, and this architecture is realized by controlled fabrication techniques. Many previous studies examining the effect of scaffold designs on chondrogenesis have not rigorously controlled scaffold design parameters like pore shape and permeability, making it difficult to assess what specific design factor had the most influence on chondrogenesis.[1–7]

On the basis of our own previous work,[8] designed polycaprolactone (PCL) scaffolds with lower permeability enhanced chondrogenesis using primary chondrocytes. However, this study examined one pore shape in PCL scaffolds and did not examine changes in scaffold/tissue construct mechanical properties with tissue ingrowth. We also have demonstrated that chondrocytes cultured in ellipsoidal pores produced more robust extracellular matrix with higher sulfated glycosaminoglycan (sGAG) concentrations in comparison to cubical pores due to increased aggregation of local chondrocytes inside each pore of poly(propylene furmarate).[1,9] However, the permeability of these scaffolds was not experimentally characterized, making it difficult to determine if permeability was significantly different between designs. Poly(1,8-octanediol-*co*-citrate) (POC) has been shown to be a good candidate for cartilage tissue engineering due to its biocompatibility, biodegradability, and mechanical properties,[10–12] yet there is no data on how POC scaffolds with rigorously controlled pore architectures (i.e., pore shape, pore size, permeability, and regular pore interconnectivity) influence chondrogenesis and how mechanical properties of POC scaffolds change with tissue development. The goal of this study was to determine how POC scaffolds with designed and rigorously controlled scaffold permeability and pore shape

Departments of [1]Biomedical Engineering, [2]Mechanical Engineering, and [3]Surgery, University of Michigan, Ann Arbor, Michigan.

influence chondrogenesis as determined by chondrogenic gene expression, matrix production, and tissue/scaffold mechanical properties. Scaffold design parameters, including permeability, pore shape, and surface area, were controlled by computational design, and control of these parameters in the final fabricated scaffolds was verified by microcomputed tomography. Additionally, since type I collagen gel was used as a cell carrier within the POC scaffolds, we determined how collagen I gel concentration affected chondrogenesis before assessments of the three-dimensional (3D) tissue/scaffold constructs.

Materials and Methods

Collagen I/hyaluronic acid hydrogel

High-concentration collagen I hydrogels and hyaluronic acid (HyA) were purchased from BD Bioscience Discovery Labs and Hyalogic LLC, respectively. High-concentration collagen I hydrogels were diluted with 0.02 N sterile acetic acid for desired concentration (9.92, 6, and 4 mg/mL) and 5% (w/w) HyA was combined with collagen I hydrogel based on our previous results showing that collagen I gel with 5% HyA enhanced chondrogenesis.

Synthesis of pre-POC

All chemicals were purchased from Sigma-Aldrich. POC pre-polymer (pPOC) was synthesized as previously described.[12] Briefly, equimolar amounts of citric acid and 1,8-octanediol were added to a 500 mL three-neck round-bottom flask fitted with an inlet and outlet adapter. The mixture was melted at 160°C–165°C for 15 min under a flow of nitrogen gas while stirring. The temperature of the system was subsequently lowered to 140°C for 40 min with constant stirring to create a pre-polymer.

Scaffold design and fabrication

To design 3D POC scaffold architectures, previously developed image-based design processes and software were used.[1,13–15] Porous POC scaffolds (6.35 mm diameter, 4.0 mm height), with 900 μm interconnected spherical or cylindrical pores (porosity: 50% spherical [S50], 62% cubical [C62]; permeability: High [C62] = Low × 13.5 [S50]) were designed using customized Interactive Design Language (IDL) programs (RSI). The details of POC scaffold fabrication were the same as previously reported.[12,15] In brief, wax molds with designed architecture were built by a Solidscape Patternmaster™ machine and inversely solid freeform-fabricated hydroxyapatite (HA) molds were prepared before curing pPOC into architecture scaffolds.[16] pPOC was poured into the wells of a Teflon mold and HA molds were embedded within the pPOC. The pPOC/HA/Teflon mold unit was cured at 100°C for 1 day followed by curing at 100°C for 3 days more with high vacuum (−30 in.Hg). The HA mold was removed by incubation in a decalcifying reagent (RDO; APEX Engineering Products) for ~6 h followed by incubation in water (Milli-Q water purification system) for 24 h to obtain the final porous POC scaffolds and POC scaffolds were dried at room temperature for ~24 h before autoclaving.

Mechanical tests

Four to six porous scaffolds or tissue grown scaffolds per each design were tested in unconfined compression (Alliance RT/30 electromechanical test frame, 50 N load cell with 0.5% error range, MTS Systems) and TestWorks4 software (MTS Systems) was used to collect data during compression testing. MATLAB (The MathWorks) software was used to fit a nonlinear elasticity model, $\sigma = A[e^{B\varepsilon} - 1]$ to experimental data, where σ is the 1st Piola-Kirchoff stress, ε is large strain, and A and B are model coefficients. The sum of least square errors between the model stress and experimental stress was minimized using the LSQNONLIN minimization program in the MATLAB optimization toolbox. Tangent moduli ($= AB e^{B\varepsilon}$) were calculated at 1%, 10%, and 30% strain from fit data and all residuals between model and experimental stress were below 1%.

Porosity and permeability measurements

Seven scaffolds per material were scanned in air using an MS-130 high-resolution microcomputed tomography scanner (GE Medical Systems) at 19 μm voxel resolution, at 75 kV and 75 mA. The porosity of each specimen was calculated by defining a region of interest that encompassed the entire scaffold and an appropriate threshold level was applied to delineate the solid scaffold material using GEMS Microview software (GE Medical Systems). All porosity scanning was performed before mechanical tests to avoid any artifacts due to compression. Scaffold permeability ($N = 6$–7, each material) with and without composite HyA/collagen I (Col I, 6 mg/mL) gel was measured using previously developed protocols on a permeability test setup.[12,17] Permeability of scaffolds with hydrogels was measured to mimic cell loading conditions *in vitro*.

Cell isolation and cell/hydrogel seeding of scaffolds

Primary porcine chondrocytes (pChon) were isolated from the joints of domestic pigs. Cartilage slices were extracted aseptically within 3 h of slaughter. Chondrocytes were isolated using a solution of 1 mg/mL collagenase II (Sigma) in Dulbecco's modified Eagle medium (DMEM) containing 500 U/mL penicillin and 500 mg/mL streptomycin (P/S), 100 U/mL kanamycin, and 1:500 amphotericin B (Fungizone; Gibco). The tissue was digested for 5 h at 37°C with gentle agitation. The cell suspension was filtered through a nylon sieve (70-mm pore size) and the centrifuged cell pellets were re-suspended in the basal culture medium (DMEM, 10% fetal bovine serum, 1% P/S, Gibco) supplemented with 50 mg/mL 2-phospho-L-ascorbic acid (Sigma) and plated onto tissue culture flasks. Cells were allowed to adhere for ~24 h and trypsinized for *in vitro* culture.

Harvested chondrocytes were seeded into 3D scaffolds by first suspending the cells in media with composite HyA/Col I gels and then pushing the gel into the 3D scaffolds.[1] Collagen I gels were used as a cell carrier for POC scaffolds to provide better cell distribution within scaffold pores. Five percent HyA was added to provide a favorable environment for chondrocyte differentiation/proliferation based on our previous work.[1] The gelation procedure was as follows: 770 μL of Col I (stock concentration: 9.92, 6, or 4 mg/mL; BD Bioscience Discovery Labs) with 77 μL HyA (stock concentration: 3 mg/mL in 1.5 M sodium chloride [NaCl], molecular weight 2.4–3 million Da; Hyalogic LLC) were well-mixed. The pH of the HyA/Col I suspension was increased with the addition of 11 μL of 0.5 N sodium hydroxide with 220 mg/mL

sodium bicarbonate to initiate gelation. As soon as 0.5 N sodium hydroxide is added to HyA/Col I gel mixture, gel contents were evenly re-suspended. Hydrogel mixtures were then dripped down onto pre-prepared sterile scaffolds until scaffolds were fully soaked and filled with gel to the top surface. This was followed by incubation at 37°C for 30 min to solidify gels further. Roughly, 121 and 150 μL of cell/gel mixtures were used for 50% and 62% porous scaffolds, respectively, to keep the same cell density per volume.

In vitro *cell culture and histology*

pChon were seeded onto scaffolds following the methods previously published with some modifications.[1] In short, cells were re-suspended at a density of $\sim 30\times10^6$ cells/mL in 770 μL of composite HyA/Col I with $\sim$50 μL of culture medium. The remaining steps were the same as previously described (see Mechanical tests section). Scaffolds seeded with pChon were cultured with the chondrogenic medium (basal medium [DMEM, 10% fetal bovine serum, and 1% P/S; Gibco] supplemented with 50 mg/mL 2-phospho-L-ascorbic acid [Sigma], 0.4 mM proline [Sigma], 5 mg/mL insulin [Gibco], and 0.1 mM nonessential amino acids [Gibco]) in 12-well plates. Chondrocytes were cultured for 0 (1 day), 2, or 4 weeks under gentle agitations on an orbital shaker and the medium was changed every other day. All POC scaffolds were sterilized in an autoclave and presoaked in DMEM for 24 h and briefly rinsed with phosphate-buffered saline (PBS) before cell seeding. Cell culture was maintained in a water-jacket incubator equilibrated with 5% CO_2 at 37°C. For histology, constructs ($N=3$/material) at each time point were fixed in 10% buffered formalin overnight, dehydrated with a series of graded ethanol, and embedded in paraffin. Tissue sections were stained with safranin O/Fast Green counterstaining to assess cell distribution, morphology, and sGAG production. Eight to 10 slides (four sections/slide) were obtained from the center of each scaffold (top to bottom and left to right).

sGAG and DNA quantification

For comparing the effects of collagen I gel concentration on chondrocytes, at 7 days sGAG and DNA contents of collagen/cell hydrogels ($N=4$–5/concentration) were quantified using the same methods as for scaffolds. At 2 and 4 weeks, scaffolds ($N=8$) at each time point or each design were removed from culture, finely diced, and placed immediately into 1 mL of pre-prepared papain solution (papain [10 units/mg: Sigma Aldrich #P4762], 1×PBS, 5 mM cysteine HCL, 5 mM ethylenediaminetetraacetic acid, pH = 6.0; mixed for 2 h at 37°C and then filtered). Scaffolds were digested in papain solution for 24 h at 60°C then immediately stored at −20°C. The digested tissue-scaffold solution was analyzed by a dimethylmethylene blue assay. Briefly, 10 μL of sample was mixed with 200 μL of dimethylmethylene blue reagent and absorbance was read on a plate reader (MultiSkan Spectrum; Thermo) at 525 nm. A standard curve was established from chondroitin 6-sulfate from shark (Sigma, C4384) to compare absorbance for samples.[18,19] The total sGAG were normalized by DNA content, which was measured using Hoechst dye 33258 methods (Sigma, #DNA-QF). In brief, 10 μL digested sample was added to 200 μL pre-prepared Hoechst solution and read with excitation at 355 nm and emission at 460 nm (Fluoroskan Ascent FL; Thermo) in a 96-well plate. Readings were compared to standard curves made from calf thymus DNA (Sigma, #DNA-QF).[20]

Quantitative-polymerase chain reaction

Cartilage-specific gene (Type II collagen and aggrecan), chondrocyte de-differentiation marker gene (Type I and X collagen), and glycerol-dehyde-3-phosphate dehydrogenase (GAPDH) gene expression levels were determined by quantitative polymerase chain reaction (qtPCR) using a Gene Amp 7700 sequence detection system (Applied Biosystems). For different concentrations of collagen gels ($N=4$–5), only Type II and I collagens and aggrecan gene expressions were quantified with normalization with GAPDH at 7 days. Collagen hydrogels or scaffolds ($N=8$–10/design) at each time point were removed from culture, briefly rinsed with PBS, chopped into smaller pieces, and then placed into RNAlater (Qiagen). Scaffolds immersed in RNAlater were kept at 4°C for 24 h and stored at −20°C until analysis. Total RNA was extracted using an RNeasy Mini Kit (Qiagen) and reverse transcription was carried out using the SuperScript First-Strand synthesis kit (Invitrogen). A positive standard curve for each primer was obtained by qtPCR with serially diluted cDNA sample mixtures. Samples were prepared using a TaqMan universal PCR master mix (Applied Biosystems) and custom-designed porcine primers. The level of gene expressions was calculated with standard samples and normalized with GAPDH or/and low permeable design (S50).

Statistical analysis

Data are expressed as mean ± standard deviation. The statistical significance among different materials was calculated using linear regressions and one-way ANOVA with *post-hoc* comparison (Tukey) or Student's *t*-test using SPSS software (SPSS for Windows, Rel 14.0. 2005 Chicago: SPSS). Data were taken to be significant when a *p*-value of 0.05 or less was obtained.

Results

Collagen I gel concentration effects on chondrogenesis

Before examining the design effects of scaffolds on chondrogenesis *in vitro*, we wanted to optimize the microenvironment conditions for cells to grow in 3D POC scaffold. Previously, the effects of HyA combined with collagen I gel have been elucidated in our lab,[1] yet the effects of collagen I gel concentration on chondrogenesis using chondrocytes have not been studied. As our goal for this study was to provide a favorable microenvironment for chondrocytes to form cartilage tissues in our 3D scaffolds, the effects of collagen I gel concentrations on chondrogenesis were in terms of matrix production and the messenger RNA expression relevant to chondrogenesis.

When comparing 4, 6, and 9.92 mg/mL collagen I gel concentrations (Fig. 1a), there was a significant difference in terms of matrix production between 6 and 9.92 mg/mL only with 6 mg/mL Col I gel supporting formation of the highest amount of matrix. However, in gene expression, lower concentrations of Col I gels caused less de-differentiation indicated by an increasing trend of the ratio of collagen 2 gene expressions to collagen 1 gene expression of cells (Col2/

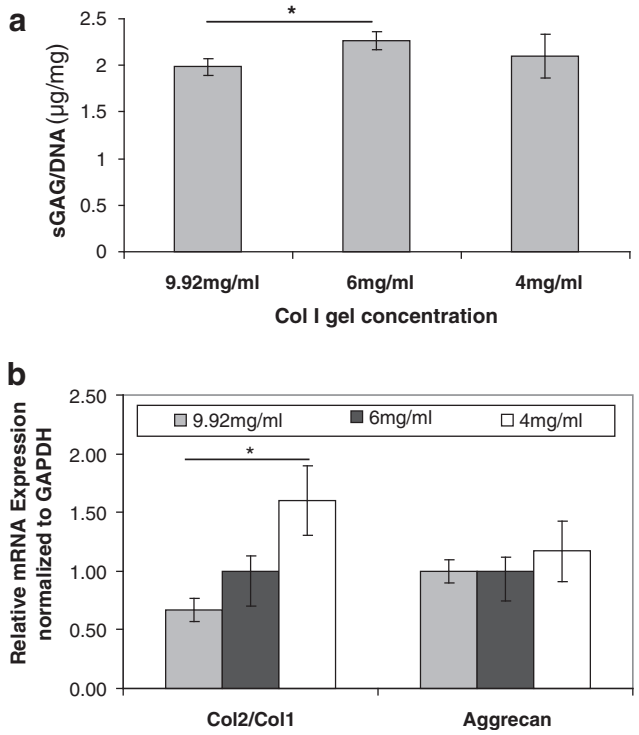

FIG. 1. The effects of collagen I gel concentration on porcine chondrocytes for 7 days. **(a)** The content of sGAG/DNA represents the overall matrix production for different concentrations of collagen I gels ($N = 4$–5, $p \leq 0.05$, one way ANOVA). **(b)** Relative mRNA expression is normalized to endogenous GAPDH for different collagen I gel concentrations ($N = 4$–5, $p \leq 0.05$, one way ANOVA). sGAG, sulfated glycosaminoglycan; ANOVA, analysis of variance; GAPDH, glycerol-dehyde-3-phosphate dehydrogenase.

Col1), known as chondrocyte differentiation index (DI)[21] (Fig. 1b). Aggrecan expression was not affected significantly by Col I concentration although the 4 mg/mL concentration showed the highest aggrecan expression among three different concentrations. Overall, 4 mg/mL seemed to be the best concentration out of three concentrations and our results showed that lower Col I gel is preferred by chondrocytes in terms of differentiation. However, the gelation time of 4 mg/mL collagen I gel was too long to keep cells evenly distributed from top to bottom (cells tended to sink down at the bottom before complete gelation); thus, we decided to use 6 mg/mL instead of 4 mg/mL still for evenly distributed cell seeding in 3D POC scaffolds.

Scaffold design, fabrication, and mechanical characterization

Three-dimensional scaffolds were fabricated from POC, which imparted variations in pore shape (either spherical or cubical) while maintaining a consistent pore size and a regular interconnectivity (Table 1). Example scaffolds are shown in Figure 2. For description purposes, the scaffolds with a cubical pore design and 62% porosity are labeled C62, and the scaffolds with a spherical pore design and 50% porosity are labeled S50. By varying pore shape and porosity, fabricated scaffold permeability was significantly different between designs (Low $= 3.51 \pm 0.95 \times 10^{-7}$ m^4/(N s) [S50], High $= 47.4 \pm 1.15 \times 10^{-7}$ m^4/(N s) [C62, 13.6×Low] [t-test, $p \leq 0.05$]). With collagen I/HyA hydrogel, scaffold permeability values all decreased from the original scaffold permeability as expected yet continued to exhibit a similar trend between designs (Low, High = 2.4×Low). Since collagen gels degrade typically in a week, permeability without gel most likely represents the permeability of scaffolds at 2–4 weeks without tissue ingrowth, whereas permeability with gel represents the scaffolds at 0 week with initial cell seeding. Thus, permeability is dynamically changing within the 4-week period. However, it is likely that the trend of different permeability between the different designs remains.

Table 1. Scaffold Descriptions

Design name (N = 8)	*S50, Low*[a]	*C62, High*[a]
Porosity (%)	50 ± 1.62	62 ± 2.36
Permeability without gel (10^{-7} m^4/[N s])[b]	3.51 ± 0.95	47.4 ± 1.15
Permeability with gel (10^{-7} m^4/[N s])[b]	1.72 ± 0.45	4.14 ± 0.73
Surface area (mm^2)[c]	288 ± 38	243 ± 15
Pore shape	Spherical	Cubical
Pore size	900 μm	900 μm

[a]Note that design names are based on its pore shape and porosity; for example, "S" in S50 is from "spherical pore shape" and "50" indicates its porosity. It is the same for C62, with "C" from "cubical pore shape." Low and high are based on relative permeabilities.
[b]Statistically significant ($p \leq 0.05$, t-test).
[c](Not Significant (NS), $p \leq 0.05$, t-test).

Table 2a and b summarize the nonlinear model fit coefficients and compressive tangent moduli for different scaffold designs. As Figure 3a shows, the more porous scaffold exhibited the lower stiffness due to reduction of the elastic POC to provide load support. These results are consistent with reported theoretical bounds on porous nonlinear elastic materials, which demonstrate that the nonlinear stress–strain

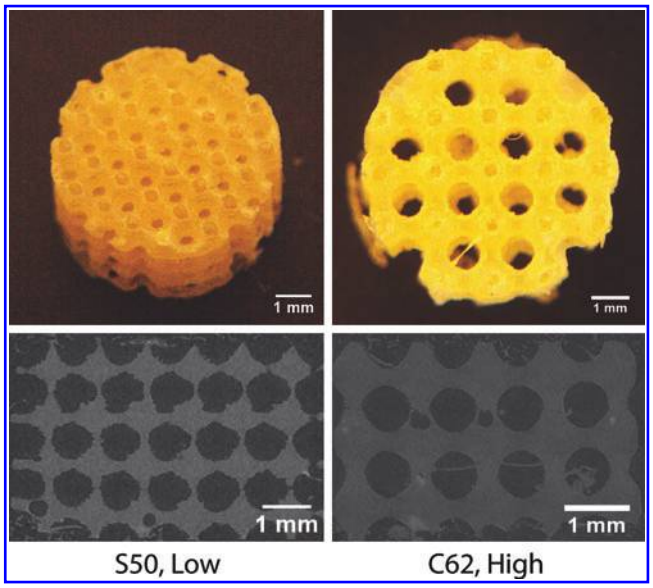

FIG. 2. Optical (top) and microcomputed tomography (bottom) images (side view) of two different scaffold designs. Color images available online at www.liebertonline.com/ten.

TABLE 2A. $\sigma = A(e^{Be} - 1)$ NONLINEAR MODEL FIT COEFFICIENTS AND TANGENT MODULI

Empty scaffolds	*Nonlinear model coefficients*		
Design/coefficients	*A*	*B*	*fval*
S50	0.11 ± 0.03	1.89 ± 0.36	8.88E-04
C62	0.013 ± 0.004	4.34 ± 0.58	6.92E-04

fval is value of the objective function: [objective function = $(\sigma^{\text{experiment}} - \sigma^{\text{model fit}})^2$].

TABLE 2B. TANGENT MODULI (MPA) AT 1%, 10%, AND 30% STRAIN

Design/strain (%)	*1*	*10*	*30*
S50	0.199 ± 0.010	0.235 ± 0.004	0.344 ± 0.019
C62	0.057 ± 0.014	0.085 ± 0.021	0.201 ± 0.048

curve of the base material is an upper bound on the nonlinear stress–strain curve of the porous material.[22] In other words, the nonlinear stress–strain curve of the porous material will be contained within the nonlinear stress–strain curve of the base material. Porosity reduces the stiffness of nonlinear base materials.[23,24]

Unlike the relation between porosity and stiffness, there was no significant trend or relation between permeability and scaffold stiffness. Table 3a and b and Figure 3b–d summarize nonlinear model fit coefficients and compare compressive tangent moduli for different scaffold designs with or without cells at different time points (2 and 4 weeks). Control here represents scaffolds seeded with gels only that were subjected to the same conditions as those scaffolds seeded with cells/gels. At 2 weeks, there was no significant difference in control versus cell-seeded scaffolds (data not shown); however, at 4 weeks both designs with cells have shown a significant increase in tangent moduli compared to control scaffolds (Fig. 3b). The lower permeability (S50) scaffold design showed a higher increase ($\sim$10 times) in tangent moduli from control and this is probably due to the faster tissue formation rate over scaffold degradation rate compared to the higher permeable design (C62). As more tissue formed, the mechanical behavior became more nonlinear with higher strain stiffening. Figure 3c shows the effects of architectural scaffold design on scaffold degradation when no cells were involved; low permeability design decreased its stiffness significantly over 4 weeks but not the high permeability design. From 2 to 4 weeks, both designs increased in stiffness and nonlinearity, indicating active tissue formation inside scaffold pores in that 2-week period (Fig. 3d). Overall, Figure 3b–d suggest that tissue formation is dominant over scaffold degradation in determining overall scaffold/tissue construct mechanical properties up to 4 weeks, especially in the low permeable design.

In vitro *cell culture—matrix production and mRNA expression*

Chondrocytes proliferated and produced cartilaginous matrix during the 2 and 4 weeks *in vitro* culture periods (Fig. 4). The low permeable design (S50) attained significantly higher sGAG/DNA content at both time points and showed a significant increase of sGAG/DNA content from 2 to 4 weeks (39.62 to >55.94, $\sim$140% increase), whereas the high permeable design (C62) did not show a significant increase in matrix production from 2 to 4 weeks. An increase in sGAG/DNA content implies that a single cell is more geared toward chondrocytic phenotype with more matrix production. At 2 weeks sGAG/DNA content of S50 was 1.6 times higher than that of C62 and at 4 weeks sGAG/DNA content of S50 was 2.3 times higher than that of C62.

qtPCR was used to measure messenger RNA expression for collagens by cells and for aggrecan found in cartilage at the 4-week time point (Fig. 5). Although there were trends with other gene expression ($p \leq 0.1$), only Col2/Col1 (DI) and Col10 expression showed a statistically significant difference between the two designs ($p \leq 0.05$). The main components of healthy articular cartilage are collagens and proteoglycans, which form a highly organized network together. Type II collagen is the major fibrillar collagen of articular cartilage, accounting for 90%–95% of the overall collagen content and determining mechanical behavior[25]; hence, it is often used as a marker for cartilaginous tissues. When Type II collagen is destroyed, it is replaced with a type I collagen fibro-cartilage that does not have the same functional properties as type II collagen, and this is why DI is frequently used as a marker for chondrocytic differentiation. The low permeable design (S50) showed higher collagen 2 and lower collagen 1 expression resulting in DI to be 1.6 times higher than the DI of the high permeable design (C62).

Aggrecan is the main proteoglycan found in cartilage, and is a typical marker of differentiated chondrocytes along with collagen II. Even though aggrecan expression of both designs was not significantly different, S50 was higher than C62. Type X collagen serves as a marker of the terminally differentiated (hypertrophic) chondrocyte phenotype, and detection of the type X collagen gene transcript and translation product is useful for studies of chondrocyte growth and dedifferentiation.[26,27] Type X collagen expression of C62 was significantly higher than that of S50 (2.2 times higher than S50), implying a greater tendency to hypertrophy.

Histology

Safranin-O staining (Fig. 6) supported the sGAG quantification data such that low permeable design (S50) showed a larger area of sGAG staining overall and each pore was more packed with sGAG-containing tissues. Also, even for outer layer tissues formed around the edges of scaffolds, low permeable design had darker sGAG staining with more vivid chondrocytic cell phenotypes (i.e., round shape with lacuna) than high permeable design, consistent with the results in Figure 4.

Discussion

There are many structural parameters that characterize and affect the overall function and performance of 3D scaffolds, including pore size, porosity, pore shape, degrees of interconnectivity, and scaffold surface area. Each of these structural parameters influences permeability, and their aggregate combination determines the final permeability, a measure of effective mass transport. Because of these interrelated structural parameters, it is infeasible to isolate the

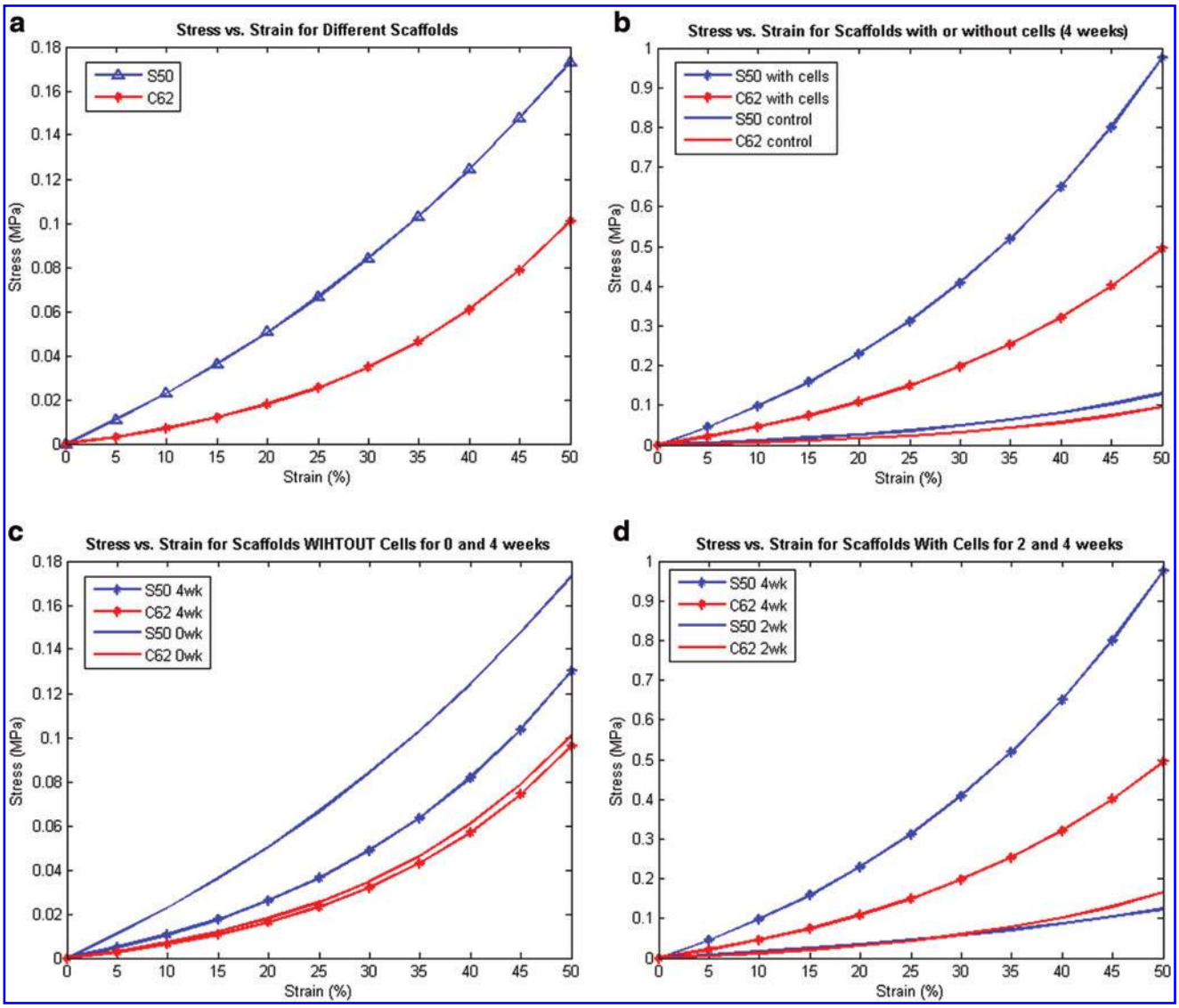

FIG. 3. **(a)** Comparison of compressive stress versus strain model fit for low (S50) and high (C62) permeable scaffold designs. **(b)** Comparison of compressive stress versus strain model fit of different scaffold designs for with or without cells (control) at 4 week time point. Control represents scaffolds that were not seeded with cells yet they were subjected to degradation by culture media over 4 weeks, whereas scaffolds with cells represent that cells were seeded onto scaffolds and were subject to both degradation and tissue formation for 4 weeks. **(c)** Comparison of compressive stress versus strain model fit for different scaffold designs at 0 and 4 week time points without cells (control). This represents a sole degradation effect on mechanical strength of the scaffolds. High permeable design (C62) causes less acid accumulation resulting in slower and less degradation overall. **(d)** Comparison of compressive stress versus strain model fit for different scaffold designs at 2 and 4 week time points with cells. More matrix formation and lower permeability reformed by tissues result in increases in mechanical strength of tissue/scaffold construct. Greater increase in stiffness of low permeable design (S50) represents more tissue formed, which is reflective of sGAG/DNA content shown in Figure 4. Color images available online at www .liebertonline.com/ten.

effects of one structural parameter on cartilage regeneration.[28] Although there have been numerous efforts to elucidate the effects of single or multiple scaffold structural parameters in cartilage tissue engineering,[3,4,29–33] they either performed limited characterization of scaffold structures and resulting permeability and mechanical properties or the architectural parameters were not rigorously designed or controlled before. Malda *et al.*,[34] Woodfield *et al.*,[5] and Miot *et al.*[35] reported the studies comparing architectures made using a bioplotter fabrication system with those created by porogen leaching and compression molding. These studies did yield insights suggesting that controlled architectures with interconnected porosity yielded increased cartilage matrix production compared to the porogen leaching method with tortuous porosity. However, the effective scaffold permeability was not characterized, neither were two well-defined pore shapes compared. Moutos *et al.*[36,37] and Valonen *et al.*[38] evaluated 3D woven textile PCL scaffolds for cartilage regeneration. They determined aggregate modulus for these structures to be in the range of 0.4–0.8 MPa, which is within the range of native articular cartilage. Permeability was determined by fitting creep data to linear biphasic the-

TABLE 3A. MODEL FIT FOR SCAFFOLDS WITH CELLS: CONTROL (GEL, NO CELL) VERSUS SCAFFOLDS (GEL + CELL) FOR 2, 4 WEEK

Scaffold design/conditions (N = 4)	*Control*		*Cells*	
	A	*B*	*A*	*B*
S50 2 week	0.003 ± 0.001	6.51 ± 1.08	0.060 ± 0.014	2.24 ± 0.41
C62 2 week	0.003 ± 0.000	6.55 ± 0.37	0.024 ± 0.027	4.13 ± 2.08
S50 4 week	0.023 ± 0.006	3.79 ± 0.23	0.28 ± 0.33	3.00 ± 1.15
C62 4 week	0.011 ± 0.005	4.55 ± 1.26	0.114 ± 0.175	3.35 ± 1.65

fval is within 0.000–0.005 so not shown.

TABLE 3B. TANGENT MODULI AT 10% STRAIN

Scaffold design (N = 4)/ *conditions*	*Control*	*Cells*
S50 2 week	0.038 ± 0.006	0.161 ± 0.005
C62 2 week	0.042 ± 0.003	0.095 ± 0.061
S50 4 week	0.125 ± 0.027	0.550 ± 0.045
C62 4 week	0.072 ± 0.002	0.156 ± 0.055

ory. Aggregate modulus increased and permeability decreased with ingrowth, similar to this study. However, cartilage gene expression was not determined and safranin O/Fast Green staining did not reveal significant sGAG content in the scaffolds. Further, permeability was not determined by direct fluid flow experiments. The variability of pore structure created by the textile weaving is not known, and therefore it is uncertain whether the pore structure is rigorously controlled as in the current study. Although permeability was measured, it was not specifically controlled through scaffold design. Lastly, we have previously shown[39] that PCL scaffolds do not support cartilage regeneration or POC scaffolds for the same architecture.

In our study, we designed scaffolds such that pore size, surface area, and degrees of interconnectivity were rigorously controlled within narrow ranges. Further, pore shape was specifically controlled to match either spherical or cubical pore geometry. Thus, the effects of porosity, pore shape, and surface area on permeability and mass transport were well characterized. In a previous study,[8] we examined the effects of scaffold permeability on chondrogenesis by varying both porosity and surface area within a spherical pore shape. This study demonstrated that scaffolds with reduced permeability improved *in vitro* chondrogenesis by primary chondrocytes. However, since permeability was decreased by changing the spherical neck connection size, lower permeable scaffolds would have increased surface area. Although we postulated that surface area was not a major factor in that study since the chondrocytes were not seen on histology to attach to the scaffold surface, it, nonetheless, raises the question whether increased surface area played a role in the increased chondrogenesis with decreased permeability.

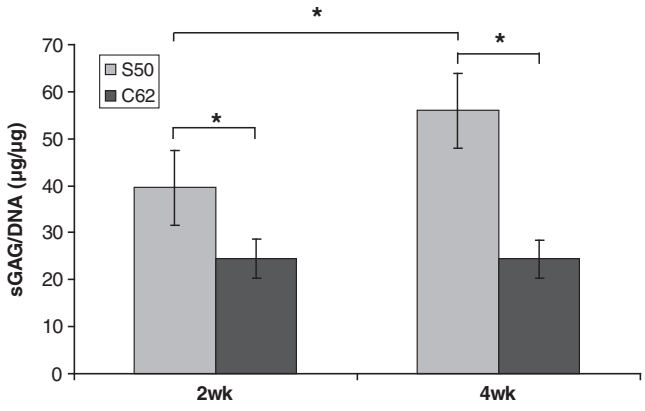

FIG. 4. The representation of matrix production for different scaffold architectures: the sGAG/DNA content was normalized to that of 0 week. ($N = 7$–8, one way ANOVA, $^*p \leq 0.05$).

In this study, we designed scaffolds to examine the effects of permeability due to pore shape while eliminating surface area as a potential confounding factor. In addition, the porosity difference between the two designs was minimal (1.2×between designs) compared to the permeability differences (13.5×between designs). Thus, in this study, we have isolated the major differences in scaffold architecture to permeability and pore shape (cylindrical vs. spherical). Since the overall impact of scaffold design on cartilage regeneration should not just be measured in terms of cartilage matrix production and gene expression, we also determined how scaffold architecture affected scaffold degradation and scaffold mechanical behavior with and without seeded cells. Scaffold behavior with seeded cells obviously represents the overall mechanics of the scaffold/regenerated tissue construct.

The lower permeable with spherical pore shape design, "S50," led to increased cartilage matrix production and increased cartilage gene expression (Figs. 4–6). The spherical pore shape may have helped creating denser cell aggregation within the pore volume, conditions that would be favorable to chondrogenesis.[9,32] In addition, as we have earlier suggested[8] that the lower permeability may enhance chondrogenesis due to decreases in oxygen tension and lower reactive oxygen species around cells that results from lower permeability and higher cell concentration. Finally, lower permeable design may demonstrate enhanced cartilage matrix production due to retained sGAG molecules that could diffuse out from more permeable designs. These three factors, (1) increased cell aggregation, (2) decreased O_2 tension resulting from lower permeability, and (3) increased sGAG retention in lower permeable designs, could all contribute to enhanced chondrogenesis in the spherical pore shapes. Thus, the spherical pore shape may enhance chondrogenesis due to its unique capability of generating a larger pore volume for cell aggregation while maintaining low permeability for sGAG retention and low O_2 tension.

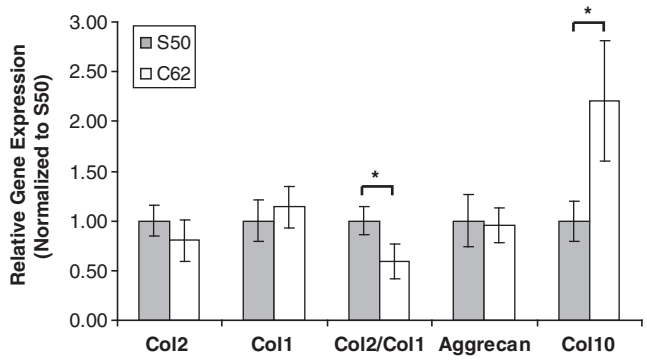

FIG. 5. Relative mRNA expression comparisons between different scaffold designs at 4 weeks ($N = 8$–10, t-test, $^*p \leq 0.05$).

In addition to significantly affecting cartilage matrix production, scaffold architecture design had significant effects on scaffold mechanics (empty without cells) and scaffold degradation (empty without cells). Architecture design significantly affected the inherent effective nonlinear elastic properties. Despite having only 12% less porosity, the stiffness of the S50 (low permeable) design as measured by tangent modulus (Fig. 3a and Table 2b) was from 1.5 to 4 times greater than the C62 (high permeable) design depending on strain magnitude. The C62 design exhibited greater nonlinear behavior, as seen in Figure 3a and as demonstrated by the larger b coefficient in the nonlinear elastic model $\sigma = A(e^{b\varepsilon} - 1)$, where a higher b coefficient indicates greater nonlinear behavior. Thus, it is clear that 3D arrangement of material greatly affects the stiffness and nonlinearity of scaffold mechanics for nonlinear elastomers like POC, even when the amount of material used in the scaffolds is very similar.

Architecture design greatly influenced *in vitro* scaffold degradation as well (Fig. 3c). The S50 design without cells demonstrated a significant decrease in effective tangent moduli, but the nonlinearity of the stress–strain curve increased. The C62 design demonstrated slight overall decrease in tangent moduli between 0 and 4 weeks, although the nonlinearity appeared unchanged. These mechanical results would suggest a significant change in polymer cross-linking and molecular weight for the S50 (Low) design, but not for the C62 (High) design. Again, given that the amount of material is similar between designs, it is likely the arrangement of material in 3D space as well as the permeability that most influenced degradation.

Of significant interest for eventual *in vivo* application are the combined effects of cartilage matrix production and scaffold material degradation on overall scaffold/tissue construct mechanical properties. Here again, there is a significant influence of scaffold architecture design. There is a tremendous increase in both the stiffness (tangent modului) and nonlinearity of both designs with seeded cells, although the increase is more dramatic for the S50 design. This reflects the greater increase in cartilaginous matrix within the S50 design over the C62 design. The tangent modulus of S50 tissue/scaffold constructs at 4 weeks (Table 3b) was also closer to the tangent modulus of native cartilage reported previously (0.44 MPa).[40] This increased cartilaginous matrix is reflected in the increased mRNA expression (Fig. 5), sGAG/DNA quantification data (Fig. 4), and sGAG staining of different scaffold designs (Fig. 6). Higher expression of collagen 2 and lower expression of collagen 1 creating a higher DI (higher collagen 2 to collagen 1 ratio), coupled with low collagen 10 expression of low permeable design (S50), are all positive indications of higher chondrocytic differentiation and matrix production, and less hypertrophy. The high permeable design (C62) seemed to cause more rapid de-differentiation marked by higher expression of collagen 1 with high tendency toward hypertrophy. Thus, in both cases, the ability to rapidly generate cartilage matrix within the pores more than overcame the material degradation effects on mechanical properties.

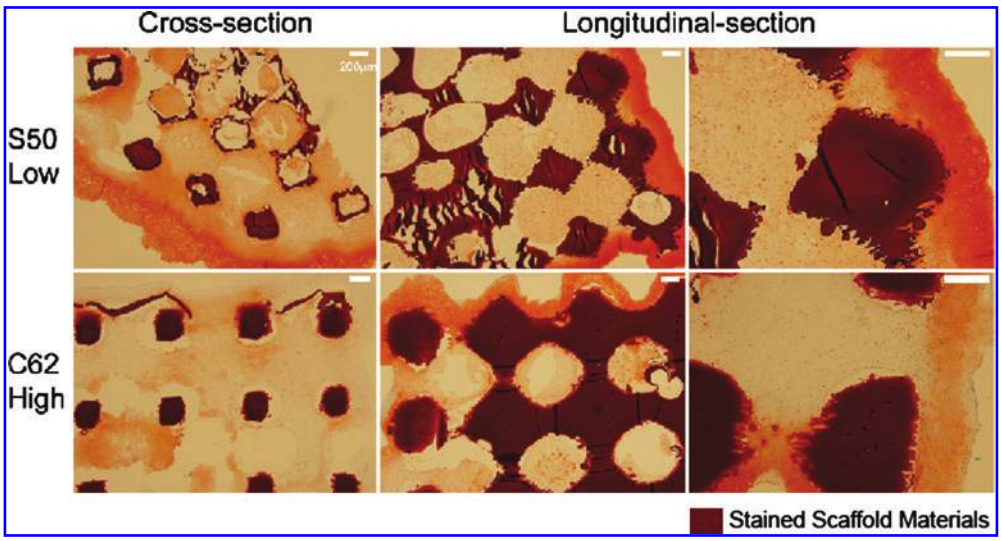

FIG. 6. Safranin-O/Fast-Green staining of scaffolds at 4 weeks: more chondrocytic cells with vivid lacunae and darker sGAG staining were present in the low permeable design with spherical pore shape (S50). All the sections were taken from the center of the scaffolds cross sectionally and longitudinally. Color images available online at www.liebertonline.com/ten.

The final component in our system that can affect cartilage matrix production is the cell seeding gel. The use of collagen gels allows seeds to be evenly seeded through the 3D architecture. Our results (Fig. 1) showed that lower collagen I gel provided a more preferable microenvironment for pChon in terms of matrix production and chondrocytic differentiation. This can be explained by comparing to the environments of chondrocytes in normal cartilage. Chondrocytes are known to be sensitive to the macromolecular organization of collagen fibrils and the spherical chondrocytes in normal cartilage are surrounded by a network of hyaluronan and GAG molecules containing Type II collagen fibrils.[41,42] The abundance of Type I collagen instead of hyaluronan, GAG, and Type II collagen surrounding chondrocytes may have led to morphological changes of chondrocytes, indicating that lower content of collagen I gel was actually better in production and maintenance of matrix (sGAG) than higher content of collagen I gel.

Conclusions

Our study clearly shows that chondrocytes prefer lower permeable scaffolds in terms of matrix production and differentiation; pore shape not only plays a role in determining effective scaffold permeability but also may play an additive role ensuring abounding pore space for enhancing cell aggregation and sGAG retention. The enhanced cartilage matrix production in the low permeable design resulted in superior mechanical properties for the scaffold/tissue construct for this design. In addition, designed pores architecture significantly influenced empty scaffold degradation kinetics in addition to effective mechanical and permeability properties. The results of this study motivate further investigation to separate pore shape and permeability effects on chondrogenesis. It further suggests that designed scaffold architecture is a component affecting the success or failure of tissue engineered cartilage that should be further studied in appropriate *in vivo* cartilage defect models.

Acknowledgments

This work was funded in part by the NIH Grant R01 AR 053379. The authors thank Gregory A. Bratkovich and Carolyn Slope for help with scaffold fabrication and cell harvest, Huina Zhang for advices with data analysis, and Chris Strayhorn for assistance with histology.

Disclosure Statement

No competing financial interests exist.

References

1. Liao, E., Yaszemski, M., Krebsbach, P., and Hollister, S. Tissue-engineered cartilage constructs using composite hyaluronic acid/collagen I hydrogels and designed poly(propylene fumarate) scaffolds. Tissue Eng **13,** 537, 2007.
2. Yamane, S., Iwasaki, N., Kasahara, Y., Harada, K., Majima, T., Monde, K., Nishimura, S., and Minami, A. Effect of pore size on *in vitro* cartilage formation using chitosan-based hyaluronic acid hybrid polymer fibers. J Biomed Mater Res Part A **81,** 586, 2007.
3. Alves da Silva, M.L., Crawford, A., Mundy, J.M., Correlo, V.M., Sol, P., Bhattacharya, M., Hatton, P.V., Reis, R.L., and Neves, N.M. Chitosan/polyester-based scaffolds for cartilage tissue engineering: assessment of extracellular matrix formation. Acta Biomater **6,** 1149, 2010.
4. Lien, S.M., Ko, L.Y., and Huang, T.J. Effect of pore size on ECM secretion and cell growth in gelatin scaffold for articular cartilage tissue engineering. Acta Biomater **5,** 670, 2009.
5. Woodfield, T.B., Malda, J., de Wijn, J., Peters, F., Riesle, J., and van Blitterswijk, C.A. Design of porous scaffolds for cartilage tissue engineering using a three-dimensional fiber-deposition technique. Biomaterials **25,** 4149, 2004.
6. Bhardwaj, T., Pilliar, R.M., Grynpas, M.D., and Kandel, R.A. Effect of material geometry on cartilagenous tissue formation *in vitro*. J Biomed Mater Res **57,** 190, 2001.
7. Yang, S., Leong, K.F., Du, Z., and Chua, C.K. The design of scaffolds for use in tissue engineering. Part I. Traditional factors. Tissue Eng **7,** 679, 2001.
8. Kemppainen, J.M., and Hollister, S.J. Differential effects of designed scaffold permeability on chondrogenesis by chondrocytes and bone marrow stromal cells. Biomaterials **31,** 279, 2010.
9. Liao, E.E. Enhancement of Chondrogenesis by Directing Cellular Condensation Through Chondroinductive Microenvironments and Designed Solid Freeform Fabricated Scaffolds. Ph.D. Thesis. Ann Arbor, MI: The University of Michigan, 2007.
10. Yang, J., Webb, A.R., Pickerill, S.J., Hageman, G., and Ameer, G.A. Synthesis and evaluation of poly(diol citrate) biodegradable elastomers. Biomaterials **27,** 1889, 2006.
11. Kang, Y., Yang, J., Khan, S., Anissian, L., and Ameer, G.A. A new biodegradable polyester elastomer for cartilage tissue engineering. J Biomed Mater Res A **77,** 331, 2006.
12. Jeong, C.G., and Hollister, S.J. Mechanical, permeability, and degradation properties of 3D designed poly(1,8 octanediol-co-citrate)(POC) scaffolds for soft tissue engineering. J Biomed Mater Res Part B **93,** 141, 2010.
13. Hollister, S.J., Maddox, R.D., and Taboas, J.M. Optimal design and fabrication of scaffolds to mimic tissue properties and satisfy biological constraints. Biomaterials **23,** 4095, 2002.
14. Hollister, S.J. Porous scaffold design for tissue engineering. Nat Mater **4,** 518, 2005.
15. Kim, K., Jeong, C.G., and Hollister, S.J. Non-invasive monitoring of tissue scaffold degradation using ultrasound elasticity imaging. Acta Biomater **4,** 783, 2008.
16. Taboas, J.M., Maddox, R.D., Krebsbach, P.H., and Hollister, S.J. Indirect solid free form fabrication of local and global porous, biomimetic and composite 3D polymer-ceramic scaffolds. Biomaterials **24,** 181, 2003.
17. Kemppainen, J.M. Mechanically Stable Solid Freeform Fabricated Scaffolds with Permeability Optimized for Cartilage Tissue Engineering. Ph.D. Thesis. Ann Arbor, MI: The University of Michigan, 2008.
18. Farndale, R.W., Buttle, D.J., and Barrett, A.J. Improved quantitation and discrimination of sulphated glycosaminoglycans by use of dimethylmethylene blue. Biochem Biophys Acta **883,** 173, 1986.
19. Chandrasekhar, S., Esterman, M.A., and Hoffman, H.A. Microdetermination of proteoglycans and glycosaminoglycans in the presence of guanidine hydrochloride. Anal Biochem **161,** 103, 1987.
20. Kim, Y.J., Sah, R.L., Doong, J.Y., and Grodzinsky, A.J. Fluorometric assay of DNA in cartilage explants using Hoechst 33258. Anal Biochem **174,** 168, 1988.
21. Martin, I., Jakob, M., Schafer, D., Dick, W., Spagnoli, G., and Heberer, M. Quantitative analysis of gene expression in

human articular cartilage from normal and osteoarthritic joints. Osteoarthritis Cartilage **9,** 112, 2001.
22. Ogden, R.W. Extremum principles in nonlinear elasticity and their application to composites. 1. Theory. Int J Solids Struct **4,** 265, 1978.
23. Hashin, Z., and Shtrikman, S. A variational approach to the theory of the elastic behavior of multiphase materials. J Mech Phys Solids **11**, 127, 1963.
24. Lopez-Pamies, O., and Idiart, M.I. An exact result for the macroscopic response of porous Neo-Hookean solids. J Elast **95,** 99, April, 2009.
25. Bruckner, P., and van der Rest, M. Structure and function of cartilage collagens. Microsc Res Tech **28,** 378, 1994.
26. Bohme, K., Conscience-Egli, M., Tschan, T., Winterhalter, K.H., and Bruckner, P. Induction of proliferation or hypertrophy of chondrocytes in serum-free culture: the role of insulin-like growth factor-I, insulin, or thyroxine. J Cell Biol **116,** 1035, 1992.
27. Shen, G. The role of type X collagen in facilitating and regulating endochondral ossification of articular cartilage. Orthod Craniofac Res **8,** 11, 2005.
28. Li, S.H., de Wijn, J.R., Layrolle, P., and de Groot, K. Accurate geometric characterization of macroporous scaffold of tissue engineering. Bioceramics **240–2,** 541, 2003.
29. Karande, T.S., Ong, J.L., and Agrawal, C.M. Diffusion in musculoskeletal tissue engineering scaffolds: design issues related to porosity, permeability, architecture, and nutrient mixing. Ann Biomed Eng **32,** 1728, 2004.
30. Yamane, S., Iwasaki, N., Kasahara, Y., Harada, K., Majima, T., Monde, K., Nishimura, S.I., and Minami, A. Effect of pore size on *in vitro* cartilage formation using chitosan-based hyaluronic acid hybrid polymer fibers. J Biomed Mater Res A **81,** 586, 2007.
31. Moroni, L., de Wijn, J.R., and van Blitterswijk, C.A. 3D fiber-deposited scaffolds for tissue engineering: influence of pores geometry and architecture on dynamic mechanical properties. Biomaterials **27,** 974, 2006.
32. Izquierdo, R., Garcia-Giralt, N., Rodriguez, M.T., Caceres, E., Garcia, S.J., Gomez Ribelles, J.L., Monleon, M., Monllau, J.C., and Suay, J. Biodegradable PCL scaffolds with an interconnected spherical pore network for tissue engineering. J Biomed Mater Res Part A **85,** 25, 2008.
33. Yen, H.J., Hsu, S.H., Tseng, C.S., Huang, J.P., and Tsai, C.L. Fabrication of precision scaffolds using liquid-frozen deposition manufacturing for cartilage tissue engineering. Tissue Eng Part A **15,** 965, 2009.
34. Malda, J., Woodfield, T.B., van der Vloodt, F., Wilson, C., Martens, D.E., Tramper, J., van Blitterswijk, C.A., and Riesle, J. The effect of PEGT/PBT scaffold architecture on the composition of tissue engineered cartilage. Biomaterials **26,** 63, 2005.
35. Miot, S., Woodfield, T., Daniels, A.U., Suetterlin, R., Peterschmitt, I., Heberer, M., van Blitterswijk, C.A., Riesle, J., and Martin, I. Effects of scaffold composition and architecture on human nasal chondrocyte redifferentiation and cartilaginous matrix deposition. Biomaterials **26,** 2479, 2005.
36. Moutos, F.T., and Guilak, F. Functional properties of cell-seeded three-dimensionally woven poly(epsilon-caprolactone) scaffolds for cartilage tissue engineering. Tissue Eng Part A **16,** 1291, 2010.
37. Moutos, F.T., Freed, L.E., and Guilak, F. A biomimetic three-dimensional woven composite scaffold for functional tissue engineering of cartilage. Nat Mater **6,** 162, 2007.
38. Valonen, P.K., Moutos, F.T., Kusanagi, A., Moretti, M.G., Diekman, B.O., Welter, J.F., Caplan, A.I., Guilak, F., and Freed, L.E. *In vitro* generation of mechanically functional cartilage grafts based on adult human stem cells and 3D-woven poly(epsilon-caprolactone) scaffolds. Biomaterials **31,** 2193, 2010.
39. Jeong, C.G., and Hollister, S.J. A comparison of the influence of material on *in vitro* cartilage tissue engineering with PCL, PGS, and POC 3D scaffold architecture seeded with chondrocytes. Biomaterials **31,** 4304, 2010.
40. Hollister, S.J. Scaffold design and manufacturing: from concept to clinic. Adv Mater **21,** 3330, 2009.
41. Farjanel, J., Schurmann, G., and Bruckner, P. Contacts with fibrils containing collagen I, but not collagens II, IX, and XI, can destabilize the cartilage phenotype of chondrocytes. Osteoarthritis Cartilage **9 Suppl A,** S55, 2001.
42. Terada, S., Yoshimoto, H., Fuchs, J.R., Sato, M., Pomerantseva, I., Selig, M.K., Hannouche, D., and Vacanti, J.P. Hydrogel optimization for cultured elastic chondrocytes seeded onto a polyglycolic acid scaffold. J Biomed Mater Res Part A **75,** 907, 2005.

Address correspondence to:
Scott J. Hollister, Ph.D.
Department of Biomedical Engineering
University of Michigan
Ann Arbor, MI 48109-2125

E-mail: scottho@umich.edu

Received: May 19, 2010
Accepted: July 19, 2010
Online Publication Date: September 14, 2010

This article has been cited by:

1. Christopher J. Bettinger. 2011. Biodegradable Elastomers for Tissue Engineering and Cell-Biomaterial Interactions. *Macromolecular Bioscience* n/a-n/a. [CrossRef]